The possibility of a metal insulator transition in antidot arrays induced by an external driving

A. Iomin and S. Fishman
Department of Physics, Technion, Haifa 32000, Israel

August 22, 2013

Abstract

It is shown that a family of models associated with the kicked Harper model is relevant for cyclotron resonance experiments in an antidot array. For this purpose a simplified model for electronic motion in a related model system in presence of a magnetic field and an AC electric field is developed. In the limit of strong magnetic field it reduces to a model similar to the kicked Harper model. This model is studied numerically and is found to be extremely sensitive to the strength of the electric field. In particular, as the strength of the electric field is varied a metal – insulator transition may be found. The experimental conditions required for this transition are discussed.

PACS numbers: 05.45.+b, 03.65.Sq, 73.23.-b

Transport phenomena of a two dimensional electron gas embedded in a periodic potential (antidot array) attracted much attention in theoretical and experimental studies [1, 2]. Investigations of magnetotransport [2, 3] and photo–conductivity [4] for GaAs heterostructures show that the electronic dynamics is essentially nonlinear with possible transition to a chaotic regime [1, 2]. Exploration of some chaotic systems illuminates a deep connection between the electron transport phenomena and quantum and classical chaos [1, 2, 5]. Specifically, the kicked Harper model (KHM) is an example of a system which is chaotic in the classical limit. It has been introduced theoretically in the field of quantum chaos because of its interesting spectral and transport phenomena. It is defined by the Hamiltonian

$$\mathcal{H}^{KH} = L_H \cos p + K_H \cos q \sum_n \delta(t-n). \tag{1}$$

The model and its variants appear naturally for the kicked harmonic oscillator [6, 7]. It is of specific interest since it does not follow the KAM picture. Its dynamics corresponds to kicks combined with rotations of the four-fold symmetry. This system exhibits chaotic motion in a region that increases with L_H and K_H. The model was subject to extensive theoretical studies [2],[6]–[10]. For some regimes of parameters its spectrum of quasi-energies is similar in nature to the energy spectrum of the Harper model [2, 9, 11, 12]. It exhibits classical and quantum diffusion as well as localization and anomalous diffusion and even ballistic motion [6]–[10]. The motivation for the explorations of the kicked Harper model in the field of quantum chaos was so far mainly theoretical, because of the variety of interesting phenomena that were found. Since the system can be modeled approximately by the kicked harmonic oscillator it can be realized experimentally [13]. Nevertheless, it has been shown recently that this system and models associated with KHM may be realized in experiments on cyclotron resonance [14]. It was proposed there that the KHM can be used to model some aspects of electronic motion in antidot arrays. In this paper we show that a family of models associated with KHM is relevant for cyclotron resonance experiments [4] in antidot arrays for some conditions.

The one particle Hamiltonian describing electrons in external fields and in a periodic potential is

$$H = \frac{1}{2m^*}\Big(\mathbf{p} - \frac{e}{c}\mathbf{A}(\mathbf{r},t)\Big)^2 + V(\mathbf{r}), \tag{2}$$

where $\mathbf{p} = (p_x, p_y)$ is the two dimensional momentum of an electron with effective mass m^* and charge e, $\mathbf{A}(\mathbf{r},t) = (\frac{c}{\nu}E_x \sin\nu t, xB - \frac{c}{\nu}E_y \cos\nu t, 0)$ is the vector potential in such a gauge that takes into account a constant magnetic field in the z–direction $\mathbf{B} = (0,0,B)$ and an alternating electric field $\mathbf{E} = (-E_x \cos\nu t,\ E_y \sin\nu t)$

with a frequency ν, while $V(\mathbf{r}) = V(x,y)$ is a two dimensional periodic potential modeling the antidot structure. For simplicity the potential

$$V(\mathbf{r}) = V_x \cos\frac{2\pi x}{a} + V_y \cos\frac{2\pi y}{b}, \tag{3}$$

where $a,\ b$ are periods in the x and y directions, will be considered, although it should be much sharper and contain more Fourier components for the antidot lattice [2]-[5]. The equations of motion for (2) are

$$\dot{p}_x = \omega^*(p_y - \omega^* m^* x + \frac{e}{\nu}E_y \cos\nu t) - \frac{\partial V(x,y)}{\partial x}, \quad \dot{x} = \frac{p_x}{m^*} - \frac{e}{m^*\nu}E_x \sin\nu t,$$
$$\dot{p}_y = -\frac{\partial V}{\partial y}, \quad \dot{y} = \frac{p_y}{m^*} - \omega^* x + \frac{e}{m^*\nu}E_y \cos\nu t, \tag{4}$$

where $\omega^* = \frac{eB}{m^* c}$ is the electronic cyclotron frequency. The following change of variables $y = \tilde{y} + y_0 \sin\nu t$ with $y_0 = \frac{eE_y}{m^*\nu^2}$ is useful. The equations of motion for the y component in terms of this variable are

$$\dot{\tilde{y}} = \frac{p_y}{m^*} - \omega^* x, \quad \dot{p}_y = -\frac{\partial V(x,y)}{\partial \tilde{y}}. \tag{5}$$

The fact that $\frac{\partial}{\partial y} = \frac{\partial}{\partial \tilde{y}}$ was used. Analogously, we make change of variables $p_x = \tilde{p}_x + \frac{e\omega^*}{\nu^2}E_y \sin\nu t$, leading to

$$\dot{\tilde{p}}_x = \omega^*(p_y - x\omega^* m^*) - \frac{\partial V(x,y)}{\partial x}, \quad \dot{x} = \frac{1}{m^*}(\tilde{p}_x + \frac{\omega^* e}{\nu^2}E_y \sin\nu t - \frac{e}{\nu}E_x \sin\nu t). \tag{6}$$

If the amplitudes $B,\ E_x,\ E_y$ satisfy

$$\frac{\omega^*}{\nu}E_y = E_x, \tag{7}$$

the equation of motion for x is particularly simple and reduces to $\dot{x} = \tilde{p}_x/m^*$. The equations of motion (5),(6) result from the effective Hamiltonian

$$\mathcal{H} = \frac{1}{2m^*}[p_x^2 + (p_y - \omega^* m^* x)^2] + V_x \cos\frac{2\pi x}{a} + V_y \cos\Big(\frac{2\pi}{b}(y + y_0 \sin\nu t)\Big)$$
$$\equiv \mathcal{H}_0(p_x, p_y, x) + V(x,y,t). \tag{8}$$

The tilde is omitted in (8) and in what follows for the sake of simplicity of notation. Here $\mathcal{H}_0 = \mathcal{H}_0(p_x, p_y, x)$ corresponds to the integrable system describing the cyclotron motion, while $V = V(x,y,t)$ is the perturbation leading to classical chaos.

As the Hamiltonian $\mathcal{H}$ is periodic in time with the period $T = \frac{2\pi}{\nu}$ the following quantum mechanical analysis will be carried out in the framework of the Floquet theory. The eigenvalue problem of the Floquet operator

$$\hat{F} = -i\hbar\frac{\partial}{\partial t} + \hat{\mathcal{H}}_0 + \hat{V} = \hat{F}_0 + \hat{V} \tag{9}$$

is considered. An unperturbed basis of $\hat{F}_0$ is

$$|j, s, u >= \frac{\nu}{\sqrt{2\pi}} e^{-ij\nu t}|s, u > . \tag{10}$$

The wave function $|s, u >$ in the coordinate representation is [12, 15]:

$$< x, y|s, u >= \frac{1}{\sqrt{2\pi lb}} e^{iyu/b}\psi_s(\frac{x}{l} - \frac{ul}{b}), \tag{11}$$

where $l = \sqrt{\hbar c/eB}$ is the magnetic length, while $\psi_s(z) = \left[\exp(-z^2/2)/\sqrt{\sqrt{\pi}2^s s!}\right] H_s(z)$ is a parabolic cylinder function and $H_s(z)$ is the s-th Hermite polynomial. The matrix of $\hat{F}_0$ in this basis is diagonal,

$$< j', s', u'|\hat{F}_0|j, s, u >= [\hbar\omega^*(s + \frac{1}{2}) - \hbar\nu j]\delta_{s,s'} \cdot \delta_{j,j'} \cdot \delta(u - u'). \tag{12}$$

The matrix elements of $\hat{V}$ can be found with the help of the generating function of the Hermite polynomials and take the form

$$< j', s', u'|\hat{V}|j, s, u >= V_x P^+_{s',s}(\tilde{h}\alpha^{-1}) \cos(\tilde{h}u - \frac{\pi}{2}|s' - s|) \cdot \delta_{j,j'} \cdot \delta(u - u')$$
$$+\frac{V_y}{2}[P^-_{s',s}(\tilde{h}\alpha) J_{j-j'}(\kappa)\delta(u - u' + 2\pi) + (-1)^{s'-s} P^-_{s',s}(\tilde{h}\alpha) J_{j'-j}(\kappa)\delta(u - u' - 2\pi)]. \tag{13}$$

where $J_n(z)$ is the Bessel function, and

$$P^{\pm}_{s',s}(w) = e^{-\pi w/2}\sqrt{\frac{s!}{s'!}}(2\pi w)^{\frac{|s-s'|}{2}} L_s^{|s-s'|}(\pm\pi w) \tag{14}$$

for $s' > s$, while for $s' < s$ one should interchange s' and s. Here $L^k_n(z)$ are the associated Laguerre polynomials, while $\alpha = b/a$ and the effective Planck constant is $\tilde{h} = \frac{2\pi l^2}{ab} = \frac{\Phi_0}{\Phi}$. The magnetic flux quantum is $\Phi_0 = \frac{hc}{e}$ and the flux through a unit cell of the periodic structure is $\Phi = abB$. Because of the periodicity in y the allowed transitions change u only by integer multiples of 2π. This is also clear from

(13). For this reason it is convenient to express u in the form $u = 2\pi n + \vartheta$ where n is an integer while $0 < \vartheta < 2\pi$. During the evolution ϑ is constant.

The eigenstates $|\lambda, \vartheta>$ of the Floquet operator $\hat{F}$ satisfying $\hat{F}|\lambda, \vartheta >= \lambda|\lambda, \vartheta >$ are decomposed into the unperturbed basis states

$$|\lambda, \vartheta >= \sum_{n,s,j} c^j_{n,s} |j, s, n, \vartheta > . \tag{15}$$

Projecting on the state $< j, s, n, \vartheta|$ one finds that the coefficients $c^j_{n,s}$ satisfy the following equation:

$$\Big[\tilde{\lambda} + \nu j\Big] c^j_{n,s} = \tilde{L} \sum_r P^+_{s,r}(\tilde{h}\alpha^{-1}) \cos\Big[\tilde{h}(2\pi n + \vartheta) - \frac{\pi}{2}|s - r|\Big] c^j_{n,r}$$

$$+ \frac{\tilde{K}}{2} \sum_{r,j'} [P^-_{s,r}(\tilde{h}\alpha) J_{j'-j}(\kappa) c^{j'}_{n+1,r} + (-1)^{s-r} P^-_{s,r}(\tilde{h}\alpha) J_{j-j'}(\kappa) c^{j'}_{n-1,r}] \tag{16}$$

The following change of variables was used here: $\nu/\omega^* \to \tilde{h}\nu$ and $\tilde{h}\tilde{\lambda} = [\lambda - \hbar\omega^*(s + \frac{1}{2})]/[\hbar\omega^*]$, while $\tilde{L} = \sqrt{\frac{V_x}{V_y}} \cdot \mathcal{K}$, and $\tilde{K} = \sqrt{\frac{V_y}{V_x}} \cdot \mathcal{K}$. The parameter $\tilde{h}\mathcal{K} = \sqrt{V_x V_y}/\hbar\omega^*$ is the strength of the coupling of the Landau bands introduced in [12] for a stationary problem of Hall conductance in this system. In the case when it is not too large ($\mathcal{K} \leq 6$) the coupling between the Landau bands is weak [12]. In the quantum case when $\tilde{h}\alpha < 1$ and $\tilde{h}\alpha^{-1} < 1$ we can neglect this interaction, i.e. the terms with $s \neq s'$ in (16) can be omitted. This can be seen from (14) since the leading term of $P_{s',s}(w)$ behaves as $w^{|s'-s|/2}$. Within this approximation (16) reduces to:

$$[\tilde{\lambda} + \nu j] c^j_n = L \cos[\tilde{h}(2\pi n + \vartheta)] c^j_n + \frac{K}{2} \sum_{j'} J_{j-j'}(\kappa)[(-1)^{j-j'} c^{j'}_{n+1} + c^{j'}_{n-1}], \tag{17}$$

where $L = \tilde{L} P^+_{s,s}(\tilde{h}\alpha^{-1})/P^-_{s,s}(\tilde{h}\alpha)$, $K = \tilde{K}$, and $[\tilde{\lambda} + \nu j]/P^-_{s,s}(\tilde{h}\alpha) \to [\tilde{\lambda} + \nu j]$, while the index s was suppressed in the notation. The Hamiltonian

$$\hat{H}_1 = L \cos\hat{p} + K \cos(\hat{q} + \kappa \sin\nu t), \tag{18}$$

reduces to (17) in the basis $e^{ikq} e^{-ij\nu t}$, where $k = \frac{u}{2\pi} = \frac{2\pi n + \vartheta}{2\pi}$ and the canonical variables are $\hat{q}$ and $\hat{p} = -i2\pi\tilde{h}\frac{\partial}{\partial q}$ satisfying $[\hat{p}, \hat{q}] = -i2\pi\tilde{h}$. In the absence of the AC electric field $\kappa = 0$ and (18) reduces to the Hamiltonian of the Harper model. For the model of this paper the semi-classical limit $\tilde{h} \to 0$ is the limit of strong magnetic field $\Phi \to \infty$ (or $B \to \infty$). The validity of equations (17) and (18) requires $\frac{\Phi_0}{\Phi} = \tilde{h} < 1$, therefore the classical limit is meaningful for (18). This Hamiltonian was studied in

[14]. It was derived there for a model opposite to the one studied here, namely the tight binding model where the external fields can be considered as a perturbation on the lattice potential.

The driving potential $K\cos(q-\kappa\sin\nu t)$ (related to the one of (18) by a trivial shifting of time) is well known in the literature and it has been discussed in the context of the description of dynamical localization in atomic momentum transfer [16, 17]. This effect has been observed experimentally following an extension of a theoretical proposal [18]. The Hamilton equations for H_1 of (18) are $\dot{q}=-L\sin p$ and $\dot{p}=K\sin\psi(t)$ with $\psi(t)=q-\kappa\sin\nu t$. For $\kappa\gg 1$ the forcing resulting in change of momentum is dominated by the resonant points [14], where $\dot{\psi}=0$ or

$$-L\sin p=\dot{q}=\kappa\nu\cos\nu t. \tag{19}$$

Expanding $\psi(t)$ around the resonant point t_r and integrating the Hamilton equation for p, taking into account the fact that this integral accumulates most of its contribution from a narrow region (of width $|\kappa\nu^2\sin\nu t_r|^{-1/2}$) around the resonance, one finds that the momentum transferred at each resonance is

$$\Delta p_r^{\pm}=\sqrt{\frac{2\pi}{\kappa\nu^2|\sin\nu t_r|}}K\sin(\psi_r^{\pm}\pm\frac{\pi}{4}), \tag{20}$$

where $\psi_r=\psi(t_r)$ and the sign depends on the direction of crossing of the resonance.

The position of the resonance depends on p. For strong driving so that $\kappa\nu\gg L$ for the resonance condition it is required that $\cos\nu t_r\approx 0$ or $|\sin\nu t_r|\approx 1$. Consequently the resonant points are $\nu t_r\approx\pm\frac{\pi}{2}$ and therefore are approximately equally spaced in time, and occur at the times: $\nu t_r^-=-\frac{\pi}{2}+2\pi l$ and $\nu t_r^+=\frac{\pi}{2}+2\pi l$ (l are integers). The resulting map is $M=M_2\cdot M_1$ with

$$\begin{aligned} M_1: &\quad \begin{cases} p_1 = & p+K_1\sin(q+\kappa_0) \\ q_1 = & q-L_1\sin p_1 \end{cases} \\ M_2: &\quad \begin{cases} p_2 = & p_1+K_1\sin(q_1-\kappa_0) \\ q_2 = & q_1-L_1\sin p_2 \end{cases} \end{aligned} \tag{21}$$

where $L_1=\frac{\pi}{\nu}L$ while $K_1=\sqrt{\frac{2\pi}{\kappa\nu^2}}K$ and $\kappa_0=\kappa-\frac{\pi}{4}$. First we note that the map is periodic in κ with the period 2π and therefore it is periodic in the magnitude of the electric field. This map is generated by the Hamiltonian:

$$\begin{aligned} \mathcal{H}_2 &= L\cos p+\nu K_1\cdot\Big[\cos(q+\kappa_0)\sum_{n=-\infty}^{\infty}\delta(\nu t+\frac{\pi}{2}-2\pi n) \\ &+ \cos(q-\kappa_0)\sum_{n=-\infty}^{\infty}\delta(\nu t-\frac{\pi}{2}-2\pi n)\Big]. \end{aligned} \tag{22}$$

In the case when $\kappa_0 = 0$ this system corresponds to the KHM. Numerical analysis shows that the model is extremely sensitive to the parameter κ_0 in both quantum ($\tilde{h} \sim 1$) and classical ($\tilde{h} = 0$) regimes. In the quantum regime we study numerically the time evolution of the variance

$$var(t) =< \hat{n}^2(t) > - < \hat{n}(t) >^2 = \sum_n n^2 |f_n(t)|^2 \tag{23}$$

and energy spreading over the unperturbed level spectrum as a result of the evolution from the initial level occupation $f_n(0)$ in the momentum space. The standard technique of the fast Fourier transform is used to evolve the quantum map (22) of the wave function over the period T over which two kicks take place: $\Psi(t+T) = \hat{U}\Psi(t)$, where $\hat{U}$ is the evolution operator over the period and $\Psi(t,q) = \frac{1}{\sqrt{2\pi}} \sum_{n=-\infty}^{\infty} e^{2\pi i n q} f_n(t)$. The initial distribution used is $f_n(0) = \delta_{n,0}$. An essential deviation from KHM is found as the parameter κ changes. The parameters K_1, L_1 and $\tilde{h}$ are the same as in [8] and are explicitly specified in the figures.

It is found here that when the parameter κ_0 is varied, localization-delocalization transition takes place, with different realizations of the delocalization as diffusion, anomalous diffusion and ballistic motion. Such a transition from diffusive motion for $\kappa_0 = 0$ to ballistic one for $\kappa_0 = g\pi$ where $g = \frac{\sqrt{5}-1}{2}$ is the golden mean is shown in Fig. 1. A localization-delocalization transition is found also for $K_1/L_1 < 2$ (see Fig. 2), such that for KHM ($\kappa_0 = 0$) there is dynamical localization of quasi-energies, while ballistic motion is found for $\kappa_0 = g\pi$. When $K_1, L_1 \ll 1$ a slow diffusive process in momentum (reported first in Ref. [8]) is observed for KHM in the semi-classical limit. It is suppressed when the parameter κ_0 increases from zero as shown in Fig. 3 resulting in transport motion in real space. This transition corresponds to a metal–insulator transition in the y-direction of the sample. Note the relation between the components of the electric field (7) that is crucial for the preference of the y direction. It is enhanced in the limit when $\tilde{h} = 0$. Numerical iterations of the classical map (21) for small values K_1 and L_1 with initial distribution taken in the vicinity of a separatrix are presented in Figs 4 and 5. These calculations demonstrate that this transport in the y direction found for finite values of κ_0 and absent when it vanishes (for the same values of K_1 and L_1) is of pure classical origin. Therefore it is expected to be robust against effects of noise.

A model for transport in a two dimensional electron gas embedded in the periodic super-lattice potential in the presence of external fields was studied. The motion corresponds to cyclotron resonance dynamics with possible metal–insulator transitions induced by the high frequency driving. It can be realized experimentally by a 2D periodic andidot array. The required conditions for experimental realization of this

effect can be achieved [4]. For $m^* \sim 0.1 m_e$, $a, b \sim 10^2 \div 4 \cdot 10^2$nm, $B \sim 0.07 \div 0.37$T, one obtains that $\omega^* \sim 10^{11} \div 5 \cdot 10^{11}\mathrm{s}^{-1}$, while $\tilde{h} \sim 0.08 \div 6$. For $\nu \sim 10^{11}\mathrm{s}^{-1}$ and $E_0 \sim 1$CGSE one obtains that $\kappa \sim 300$ and the condition $\kappa \gg 1$ is fulfilled. The amplitudes of the periodic potential can satisfy the condition $\mathcal{K} = \frac{m^* ab\sqrt{V_x V_y}}{2\pi\hbar^2} \leq 6$ for $V_x, V_y < 4$meV and $a \sim b \sim 10^2$nm. Reasonable values for the parameters of (21) and (22) are $K_1 = L_1 = 5$ that are obtained for $V_x = 0.15$meV and $V_y = 3$meV for $a = b \sim 10^2$nm, $\kappa_0 = 300$ and $\nu = 10^{11}\mathrm{s}^{-1}$. These were used in numerical calculations of the present paper. The values of K_1 and L_1 can be reduced and also numerical calculations for smaller values were performed.

Two metal–insulator transitions induced by the variation of κ_0 are predicted. The first one is a quantum effect of strong delocalization in p corresponding to anomalous (super) diffusion or acceleration for p, so that $< (\hat{p} - p_0)^2 > \sim t^\mu$ with $1 < \mu \leq 2$ for $\kappa_0 \neq 0$ and for any ratio between K_1 and L_1, while it is known that for $\kappa_0 = 0$, that corresponds to the KHM, super-diffusion takes place only for $K_1 > L_1$. It means that for $\kappa_0 \neq 0$ an initial wave packet spreads in the direction of stronger modulation of the 2D super-lattice potential. So far, in the one-band structure systems both integrable like the Harper model and chaotic like the kicked Harper model ($\kappa_0 = 0$), wave packets were found to spread in the direction of the weaker modulation of the potential amplitudes. Recently such effect has been studied in the many-band structure system with strong interaction between the bands leading to chaos in the classical limit [19]. It corresponds to electronic transport in a 2D periodic potential with different modulation amplitudes in x- and y- directions that are perpendicular to the magnetic field. The second one is a classical effect taking place for $K_1, L_1 < 1$ in the both classical $\tilde{h} = 0$ and semi-classical limit $\tilde{h} \ll 1$. It corresponds to the strong delocalization in the q direction with anomalous diffusion or ballistic motion at any ratio $\frac{K_1}{L_1}$ for $\kappa_0 \neq 0$ while for $\kappa_0 = 0$ anomalous diffusion in q takes place only when $\frac{K_1}{L_1} < 1$. This effect can be explained by the topological reconstruction of phase space due to a variation of κ_0 leading to different settling of elliptic and hyperbolic points. An analogous phenomenon has been studied for the web map [20] and it has been shown that there is a connection between the web structure and features of diffusion in phase space [10]. For the first case the quantum transition due to the non-vanishing κ_0 corresponds to delocalization in the p direction and localization in q. The second transition corresponds to delocalization in q and localization in p. Some caution is required when the model studied here is compared to antidot lattices, where the potential $V(\mathbf{r})$ in (2) should be replaced by a sharper function. In this case the equation (17) and the effective Hamiltonian (18) have more complicated form due to interaction between x and y degrees of freedom. For a sufficiently strong magnetic field, so that $\tilde{h}\alpha$ and $\tilde{h}\alpha^{-1}$ are much

smaller than unity, and $\mathcal{K} < 6$ the one Landau band approximation is valid [12] and the metal–insulator transitions considered here can be observed. (This justifies ignoring the terms with $s \neq s'$ in (13).) The result may be modified since the form of the equation corresponding to (18) may be somewhat more complicated because of the sharpness of the potential.

This research was supported in part by the Israel Science Foundation, by the U.S.–Israel Binational Science Foundation (BSF) and by the Niedersachsen Ministry of Science (Germany).

References

[1] For a review see: D. Weiss, G. Lutjering, and K. Richter, Chaos, Solitons and Fractals **8** 1337 (1997).

[2] For a review see: R. Fleischmann, T. Geisel, R. Ketzmerick, and G. Petschel, Physica **D 86**, 171 (1995).

[3] R. Fleischmann et al., Europhys. Lett. **36** 167 (1996); D. Weiss et al., Phys. Rev. Lett. **66**, 2790 (1991); R. Fleischmann, T. Geisel, R. Ketzmerick, Phys. Rev. Lett. **68**, 1367 (1992).

[4] E. Vasiliadou, *et al.*, Phys. Rev. **B 52**, R8658 (1995).

[5] R. Ketzmerick, K. Kruse, and T. Geisel, Phys. Rev. Lett. **80**, 137 (1998).

[6] G. M. Zaslavsky, M. Yu. Zakharov, R. Z. Sagdeev, D. A. Usikov, and A. A. Chernikov, Sov. Phys. JETP, 64 294 (1986); G. M. Zaslavsky, Sagdeev, D. A. Usikov, and A. A. Chernikov, Sov. Phys. Usp. **31**, 890 (1988).

[7] I. Dana, Phys. Lett. **A 197**, 413 (1995).

[8] R. Lima and D. Shepelyansky, Phys. Rev. Lett. **67**, 1377 (1991).

[9] T. Geisel, R. Ketzmerick, and G. Petschel, Phys. Rev. Lett. **67**, 3635 (1991).

[10] I. Dana and T. Horesh, in Proceedings of the Workshop on *Chaos, Kinetics, and Nonlinear Dynamics in Fluids and Plasmas*, Carry–Le–Rouet, France, 1997, edited by S. Benkadda and G. M. Zaslavsky (Springer–Verlag, Berlin, 1998); I. Dana, Phys. Rev. Lett. **73**, 1609 (1994).

[11] G. Petschel and T. Geisel, Phys. Rev. Lett. **71**, 239 (1993).

[12] D. Springsguth, R. Ketzmerick, and T. Geisel, Phys. Rev. **B 56**, 2036 (1997).

[13] S. A. Gardiner, J. I. Cirac, and P. Zoller, Phys. Rev. Lett. **79**, 4790 (1997).

[14] A. Iomin and S. Fishman, Phys. Rev. Lett. **81** 1921 (1998); Physica **D 131**, 169 (1999).

[15] D. Pfannkuche and R. R. Gerhardts, Phys. Rev. **B 46**, 12606 (1992).

[16] R. Graham, M. Schlautmann, and P. Zoller, Phys. Rev. **A 45**, R19 (1992).

[17] R. Graham, M. Schlautmann, and D. Shepelyansky, Phys. Rev. Let. **67**, 255 (1991).

[18] F. L. Moore *et al.*, Phys. Rev. Let. **73**, 2974 (1994).

[19] R. Ketzmerick, K. Kruse, D. Springsguth, and T. Geisel, cond–mat/9810313.

[20] S. Pekarsky and V. Rom–Kedar, Phys. Lett. **A 225**, 274 (1997).

Figure Captions

Fig. 1 The quantum occupation probability $|f_n(t)|$ vs n and the variance $var(t)$ found from integration of (22) for $K_1 = L_1 = 5$ and $\tilde{h} = \frac{2\pi}{7+g}$ with $\kappa_0 = 0$ (a,b) and $\kappa_0 = \pi g$ (c,d).

Fig. 2 Same as Fig. 1 but for $L_1 = 4$ and $K_2 = 2$.

Fig. 3 Same as Fig. 1 for $K_1 = L_1 = \frac{\pi}{8}$ abd $\tilde{h} = \frac{2\pi}{222+g}$ for $\kappa_0 = 0$ (a,b) and $\kappa_0 = g\pi$ (c,d).

Fig. 4 Classical evolution of the map (21) for $K_1 = L_1 = \frac{\pi}{8}$ and $\kappa_0 = 0$. Eleven trajectories are presented in figure (a) and folded to the $2\pi \times 2\pi$ torus in figure (b). The variances are presented in (c) and (d).

Fig. 5 Same as Fig. 4 but for $\kappa_0 = 0.8 \cdot g\pi$.

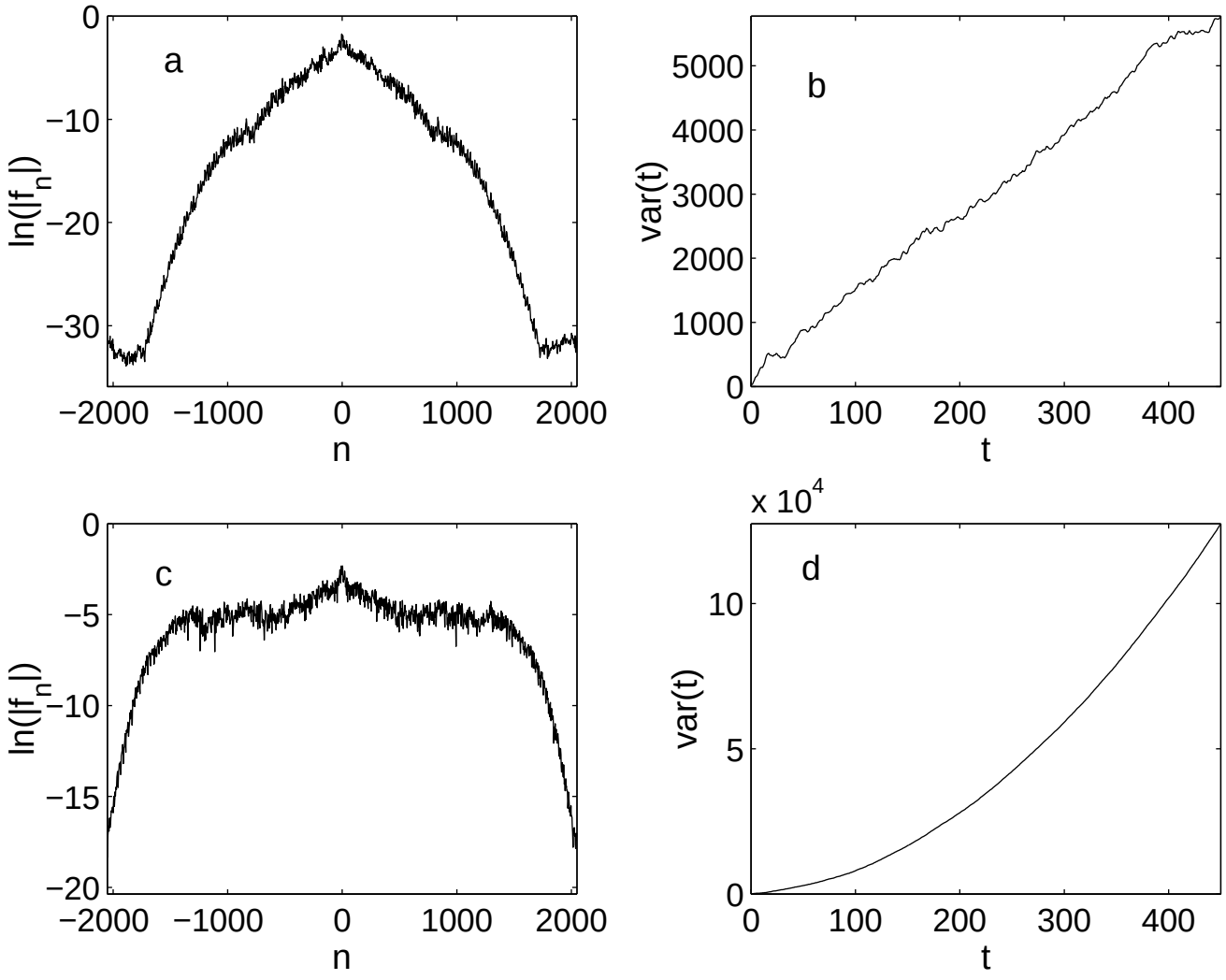
a
b
c
d
ln(|f_n|)
var(t)
n
t
x 10^4
0
−10
−20
−30
−2000
−1000
1000
2000
5000
4000
3000
100
200
300
400
−5
−15
10
5

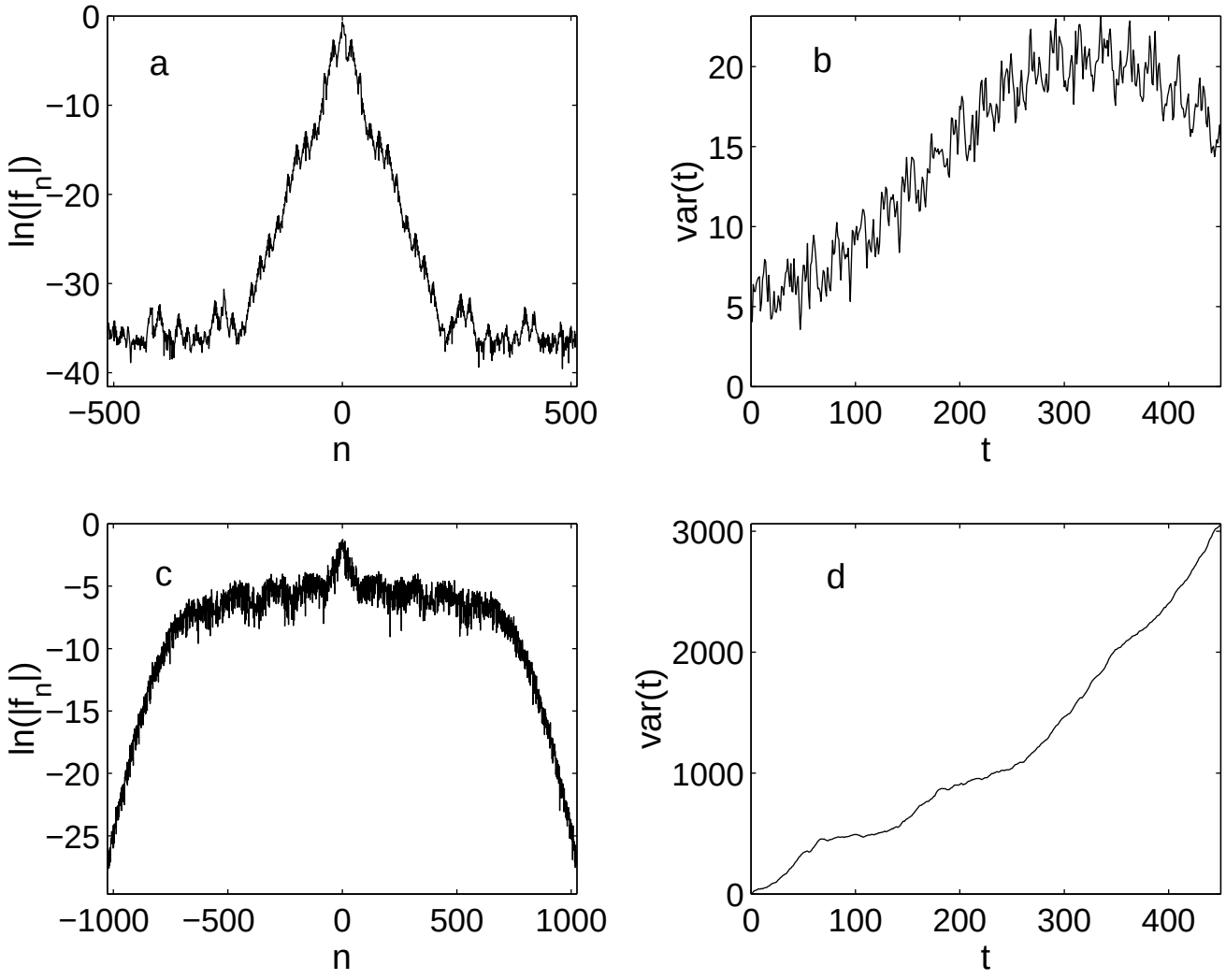
a
b
c
d
ln(|f_n|)
var(t)
n
t
0
−10
−20
−30
−40
−500
500
5
10
15
20
100
200
300
400
−5
−15
−25
−1000
1000
1000
2000
3000

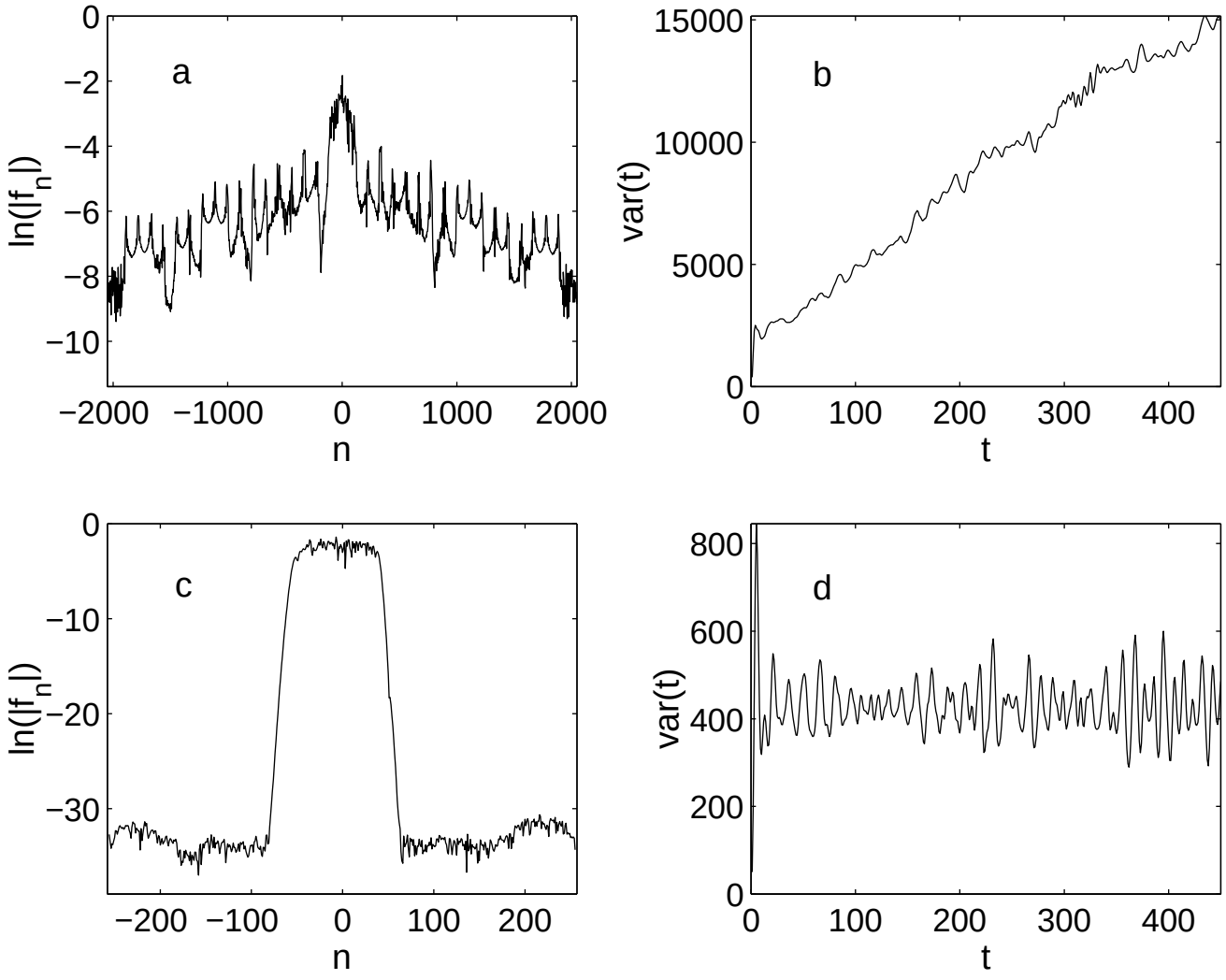
a
b
c
d
ln(|f_n|)
var(t)
n
t
0
−2
−4
−6
−8
−10
−2000
−1000
1000
2000
15000
10000
5000
100
200
300
400
−20
−30
−200
−100
800
600

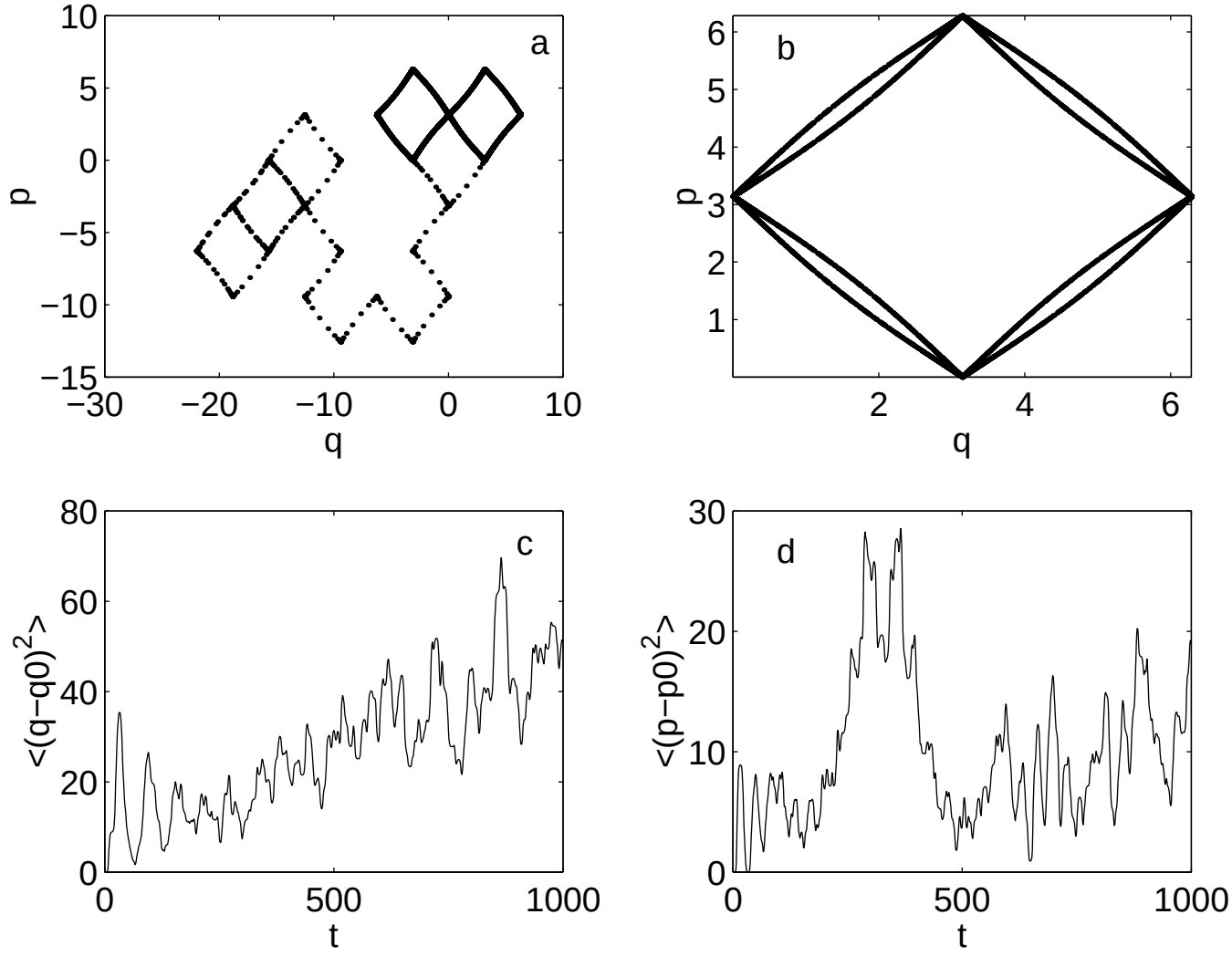
a
b
c
d
p
q
<(q−q0)^2>
<(p−p0)^2>
t
10
5
0
−5
−10
−15
−30
−20
−10
0
10
6
4
3
2
1
2
4
6
80
60
40
20
0
500
1000
30
20
10

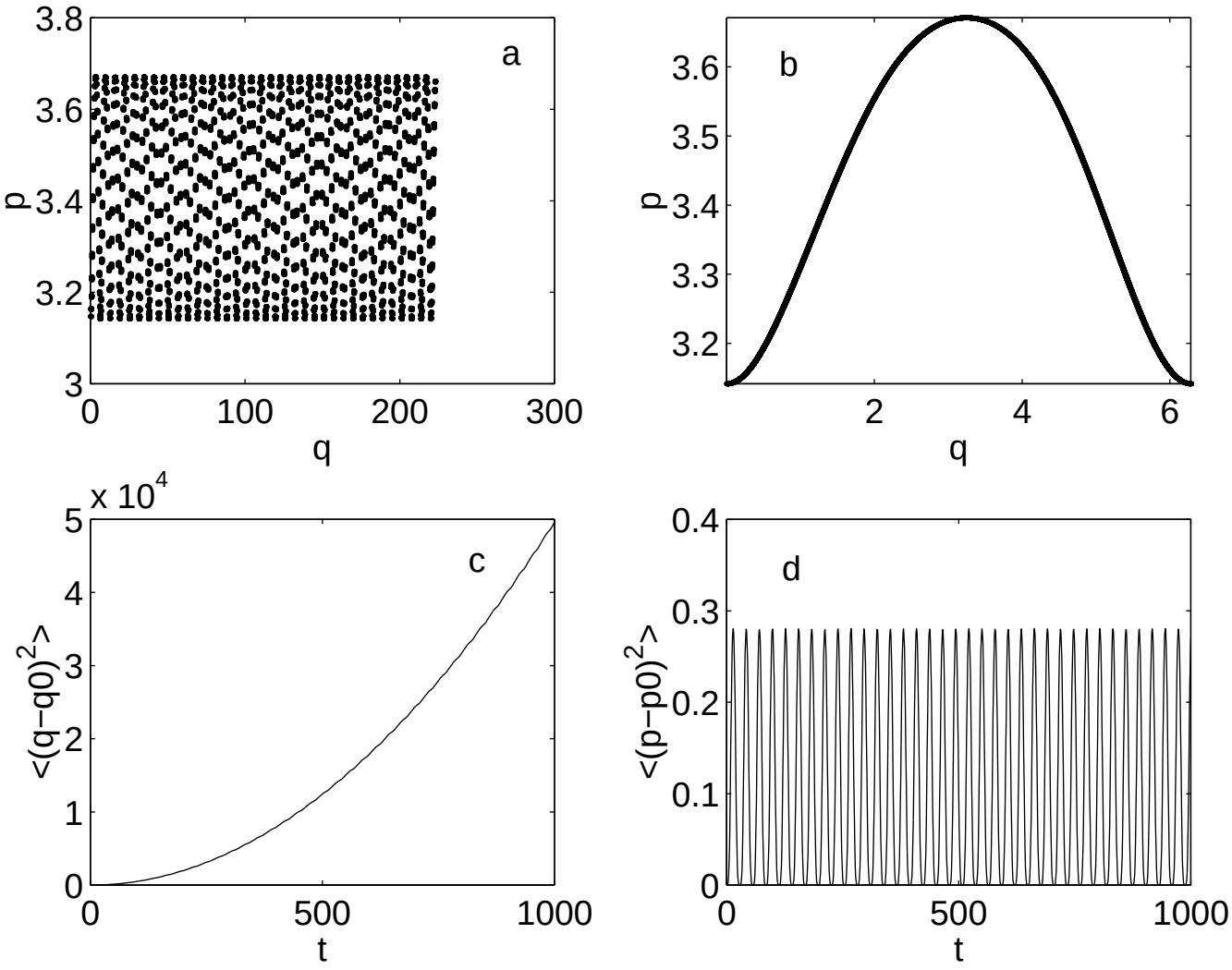
a
b
c
d
p
q
t
<(q−q0)^2>
<(p−p0)^2>
x 10^4
3.8
3.6
3.4
3.2
3
0
100
200
300
3.6
3.5
3.4
3.3
3.2
2
4
6
5
4
3
2
1
0
500
1000
0.4
0.3
0.2
0.1